应用数学和力学
APPLIED MATHEMATICS AND MECHANICS

功能梯度压电板柱面弯曲的弹性力学解

沈璐璐，蔡方圆，杨 博

Elasticity Solutions for Cylindrical Bending of Functionally Graded Piezoelectric Material Plates

SHEN Lulu, CAI Fangyuan, and YANG Bo

在线阅读 View online: https://doi.org/10.21656/1000-0887.430224 http://www.applmathmech.cn

功能梯度压电板柱面弯曲的弹性力学解*

沈璐璐，　蔡方圆，　杨　博

（浙江理工大学 建筑工程学院，杭州 310018）

（我刊编委陈伟球推荐）

摘要： 功能梯度压电材料（FGPM）同时兼具功能梯度材料和压电材料特性, 可为多功能或智能化轻质结构设计提供支撑, 在诸多领域有着广泛的应用前景. 将 Mian 和 Spencer 功能梯度板理论由功能梯度弹性材料推广到功能梯度压电材料, 解析研究了 FGPM 板的柱面弯曲问题, 其中, 材料弹性常数、压电和介电参数沿板厚方向可以任意连续变化. 最终, 给出了 FGPM 板受横向均布荷载作用下柱面弯曲问题的弹性力学解. 通过算例分析, 重点讨论了压电效应对 FGPM 板静力响应的影响.

关　键　词： 压电效应；　Mian 和 Spencer 板理论；　柱面弯曲；　弹性力学解

中图分类号： O343.1　　**文献标志码：** A　　DOI：10.21656/1000-0887.430224

Elasticity Solutions for Cylindrical Bending of Functionally Graded Piezoelectric Material Plates

SHEN Lulu，　CAI Fangyuan，　YANG Bo

（*School of Civil Engineering*, *Zhejiang Sci-Tech University*, *Hangzhou* 310018, *P.R.China*）

（Recommended by CHEN Weiqiu, M. AMM Editorial Board）

Abstract: Functionally graded piezoelectric materials (FGPMs), combining the properties of functionally graded materials and piezoelectric materials, provides a new idea for multi-functional and intelligent lightweight components, and has broad application prospects in electronic devices. Based on the elastic and electric equilibrium equations, the Mian and Spencer functionally graded plate theory was extended from elastic materials to piezoelectric materials to study the cylindrical bending of FGPM plates, where the material elastic constants, piezoelectric and dielectric parameters were assumed to vary continuously and arbitrarily along the thickness direction. Accordingly, the elasticity solutions for cylindrical bending of FGPMs plates under the uniform transverse loading were obtained. Numerical examples were given to demonstrate the piezoelectric effects on the static responses of the presented FGPMs plates.

Key words: piezoelectric effect; Mian and Spencer plate theory; cylindrical bending; elasticity solution

* **收稿日期：** 2022-07-06; **修订日期：** 2022-09-29

基金项目： 国家自然科学基金 (11872336); 机械结构强度与振动国家重点实验室开放课题 (SV2020-KF-13)

作者简介： 沈璐璐(1990—), 女, 副教授, 博士 (E-mail: lulushen@zstu.edu.cn);
蔡方圆(1998—), 女, 硕士生 (E-mail: 13588750105@163.com);
杨博(1979—), 男, 教授, 博士(通讯作者. E-mail: youngbo@zstu.edu.cn).

引用格式： 沈璐璐, 蔡方圆, 杨博. 功能梯度压电板柱面弯曲的弹性力学解[J]. 应用数学和力学, 2023, **44**(3): 272-281.

0 引 言

压电材料因其固有的力-电耦合性质而成为重要的智能材料, 目前已被制造成驱动器等智能器件, 广泛应用于各种工程领域[1]. 1987 年, 日本科学家新野正之首次提出功能梯度材料 (FGM) 这一概念[2]. 研究发现, 若将功能梯度概念引入压电材料, 形成功能梯度压电材料 (FGPM), 则压电复合材料的组分和微观结构随空间可以连续变化, 能够减缓压电复合材料中因不同材料间的不连续而造成的应力集中等问题, 从而提高器件的工作性能和使用寿命[3].

静力弯曲特性是 FGM 结构最基本的力学特性之一[4], 因此, 对 FGPM 板结构弯曲问题的研究具有重要的理论和应用价值. 例如, 边祖光[5] 基于 Soldatos 板理论, 采用层合模型和状态空间法研究了单跨或多跨正交各向异性功能梯度板的柱面弯曲行为. 基于改进的经典层合板理论, Almajid 等[6] 研究了不同类型压电致动器的应力场和平面外位移, 并用有限元模型进行了验证. Zhong 等[7] 基于弹性理论采用状态空间法给出了四边简支 FGPM 板的精确解. Navazi 等[8] 以及 Tahani 等[9] 通过引入 von Kármán 非线性应变, 研究了简支功能梯度板的非线性柱面弯曲. Wang 等[10] 基于三维压电理论, 对材料特性随厚度变化的圆板的轴对称弯曲进行了分析研究, 得到了两个不寻常边界条件的精确解和简支边界和固定边界的近似解. 仲政等[11-12] 基于弹性理论, 采用状态空间法, 获得了正交各向异性功能梯度板在上下表面荷载作用下柱面弯曲问题的 Peano-Baker 级数解. Li 等[13] 利用直接位移方法, 对功能梯度压电圆板的弯曲特性进行了研究, 并获得了自由或简支条件下的三维解析解. Li 和 Pan[14] 基于修正的耦合应力和正弦板理论, 研究了简支压电功能梯度微板的静态弯曲, 得到了机械和电荷载对位移、应力、电势的影响. Zenkour 和 Hafed[15] 基于准三维正弦剪切变形理论, 对 FGPM 板的弯曲特性进行了深入分析. Dehsaraji 等[16] 基于高阶剪切和法向可变形板理论, 利用虚功原理和变分法对 FGPM 板的柱面弯曲特性进行了研究. 王平远等[17] 基于非局部应变梯度理论[18], 研究了功能梯度纳米板结构的弯曲问题.

许多工程对象可以简化为板的柱面弯曲模型来研究[8-10,12]. 在之前的工作中, 笔者将 Mian 和 Spencer 功能梯度板理论[19] 由板上下表面无应力状态推广到了可以受横向均布荷载作用, 获得了正交各向异性功能梯度板柱面弯曲问题的弹性力学解[4]. 本文将材料由功能梯度弹性材料拓展到了 FGPM, 基于推广后的 Mian 和 Spencer 功能梯度板理论[20], 给出了横向均布荷载作用下 FGPM 板柱面弯曲的弹性力学解.

1 FGPM 板柱面弯曲的控制方程

考虑一个等厚度的 FGPM 板, 在上下表面分别作用均布荷载 q_1 和 q_2, 如图 1 所示. $0\leqslant x\leqslant l$, $-\infty<y<\infty$, $-h/2\leqslant z\leqslant h/2$, 坐标系 xOy 平面与板几何中面 ($z=0$) 重合, 此时该板处于柱面弯曲状态. 在 $z=-h/2$ 处, $\sigma_z=-q_1$, $\tau_{zx}=0$, $D_z=0$. 在 $z=h/2$ 处, $\sigma_z=-q_2$, $\tau_{zx}=0$, $D_z=0$. u 和 w 分别表示 x 方向和 z 方向的位移分量, ϕ 表示电场的电势, σ_x, τ_{zx}, σ_z, D_x, D_z 分别表示 xOz 平面上的应力和电位移分量.

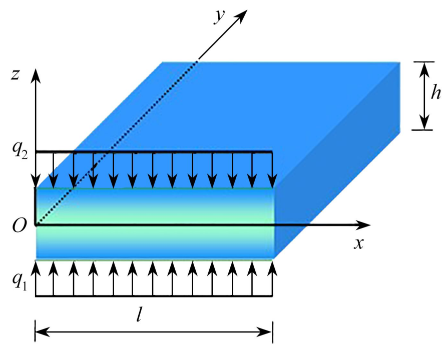

图 1 均布荷载作用下 FGPM 板示意图

Fig. 1 Schematic diagram of the FGPM plate under uniform load

针对本文研究的正交各向异性的等厚度 FGPM 板, 其在 y 方向的长度尺寸远远大于 x 和 z 方向, 在横向均布载荷作用下, 本文研究的问题便可以转化为二维平面应变问题来研究. 因此, 上述位移分量、电势、应力和电位移均与坐标 y 无关.

忽略体积力，求解该二维问题的弹性力学平衡方程为[4]

$$\sigma_{x,x}+\tau_{xz,z}=0,\ \tau_{xz,x}+\sigma_{z,z}=0. \tag{1}$$

Gauss 电平衡方程为[8]

$$D_{x,x}+D_{z,z}=0. \tag{2}$$

正交各向异性压电弹性体的本构方程为[21]

$$\sigma_x=c_{11}u_{,x}+c_{13}w_{,z}+e_{31}\phi_{,z},\ \sigma_z=c_{13}u_{,x}+c_{33}w_{,z}+e_{33}\phi_{,z},\ \tau_{zx}=c_{55}(u_{,z}+w_{,x})+e_{15}\phi_{,x}, \tag{3}$$

$$D_x=e_{15}(u_{,z}+w_{,x})-\varepsilon_{11}\phi_{,x},\ D_z=e_{31}u_{,x}+e_{33}w_{,z}-\varepsilon_{33}\phi_{,z}, \tag{4}$$

式中，c_{ij}为材料的弹性常数，e_{ij}为压电常数，ε_{ij}为介电常数，均为z的函数，即$c_{ij}=c_{ij}(z)$, $e_{ij}=e_{ij}(z)$, $\varepsilon_{ij}=\varepsilon_{ij}(z)$.

基于 Mian 和 Spencer 功能梯度板理论[4]，现寻求满足式 (1) 和 (2) 的如下形式的位移场：

$$\begin{cases}u(x,z)=\bar{u}(x)+F(z)\bar{u}_{,xx}+A(z)\bar{w}_{,x}+B(z)\bar{w}_{,xxx},\\ w(x,z)=\bar{w}(x)+G(z)\bar{u}_{,x}+C(z)\bar{w}_{,xx}+D(z).\end{cases} \tag{5}$$

参照位移场的模式，假设 FGPM 板中的电势场沿板厚按如下形式分布：

$$\phi(x,z)=\phi_1(z)\bar{u}_{,x}+\phi_2(z)\bar{w}_{,xx}+\phi_0(z). \tag{6}$$

式(5)、(6)中，$A(z)$, $B(z)$, $C(z)$, $D(z)$, $F(z)$, $G(z)$, $\phi_0(z)$, $\phi_1(z)$, $\phi_2(z)$均为待定函数.

将式 (3) 和 (4) 代入式 (1) 和 (2)，得

$$\begin{cases}\sigma_x=\bar{u}_{,x}(c_{11}+c_{13}G'+e_{31}\phi_1')+\bar{w}_{,xx}(c_{11}A+c_{13}C'+e_{31}\phi_2')+Fc_{11}\bar{u}_{,xxx}+Bc_{11}\bar{w}_{,xxxx}+D'c_{13}+e_{31}\phi_0',\\ \sigma_z=\bar{u}_{,x}(c_{13}+c_{33}G'+e_{33}\phi_1')+\bar{w}_{,xx}(c_{13}A+c_{33}C'+e_{33}\phi_2')+Fc_{13}\bar{u}_{,xxx}+Bc_{13}\bar{w}_{,xxxx}+D'c_{33}+e_{33}\phi_0',\\ \tau_{zx}=\bar{u}_{,xx}[c_{55}(F'+G)+e_{15}\phi_1]+\bar{w}_{,xxx}[c_{55}(B'+C)+e_{15}\phi_2]+\bar{w}_{,x}[c_{55}(A'+1)],\end{cases} \tag{7}$$

$$\begin{cases}D_x=\bar{u}_{,xx}[e_{15}(F'+G)-\varepsilon_{11}\phi_1]+\bar{w}_{,xxx}[e_{15}(B'+C)-\varepsilon_{11}\phi_2]+\bar{w}_{,x}[e_{15}(A'+1)],\\ D_z=\bar{u}_{,x}(e_{31}+e_{33}G'-\varepsilon_{33}\phi_1')+\bar{w}_{,xx}(e_{31}A+e_{33}C'-\varepsilon_{33}\phi_2')+e_{31}F\bar{u}_{,xxx}+e_{31}B\bar{w}_{,xxxx}+e_{33}D'-\varepsilon_{33}\phi_0'.\end{cases} \tag{8}$$

将式 (7) 和 (8) 代入式 (1) 和 (2)，并令

$$\begin{cases}[c_{55}(A'+1)]'=0,\\ c_{11}+c_{13}G'+e_{31}\phi_1'+(c_{55}(F'+G)+e_{15}\phi_1)'=c_{55}\kappa_1,\\ c_{11}A+c_{13}C'+e_{31}\phi_2'+(c_{55}(B'+C)+e_{15}\phi_2)'=c_{55}\kappa_2,\\ (c_{13}+c_{33}G'+e_{33}\phi_1')'=0,\\ c_{55}(A'+1)+(c_{13}A+c_{33}C'+e_{33}\phi_2')'=0,\\ (e_{31}+e_{33}G'-\varepsilon_{33}\phi_1')'=0,\\ e_{15}(A'+1)+(e_{31}A+e_{33}C'-\varepsilon_{33}\phi_2')'=0,\end{cases} \tag{9}$$

$$\bar{u}_{,xxx}=\kappa_3, \tag{10}$$

$$\bar{w}_{,xxxx}=\kappa_4, \tag{11}$$

式中，上标“′”表示对变量z求导数，κ_1, κ_2, κ_3和κ_4为任意常数.从而式 (1) 和 (2) 等价为

$$\kappa_1\bar{u}_{,xx}+\kappa_2\bar{w}_{,xxx}=0, \tag{12}$$

$$[c_{55}(F'+G)+(Fc_{13})'+e_{15}\phi_1]\kappa_3+[c_{55}(B'+C)+(c_{13}B)'+e_{15}\phi_2]\kappa_4+\left(c_{33}D'+e_{33}\phi_0'\right)'=0, \tag{13}$$

$$[e_{15}(F'+G)+(Fe_{31})'-\varepsilon_{11}\phi_1]\kappa_3+[e_{15}(B'+C)+(e_{31}B)'-\varepsilon_{11}\phi_2]\kappa_4+\left(e_{33}D'-\varepsilon_{33}\phi_0'\right)'=0. \tag{14}$$

由式 (10)—(12) 可得

$$\kappa_1\kappa_3+\kappa_2\kappa_4=0. \tag{15}$$

对式 (10) 和 (11) 积分可得

$$\bar{w}(x)=\frac{1}{24}\kappa_4x^4+\frac{1}{6}C_1x^3+\frac{1}{2}C_2x^2+C_3x+C_4, \tag{16}$$

$$\bar{u}(x)=\frac{1}{6}\kappa_3x^3-\frac{1}{2}\frac{\kappa_2}{\kappa_1}C_1x^2+C_5x+C_6, \tag{17}$$

式中$C_i\,(i=1,2,\cdots,6)$为积分常数，由边界条件确定.

现考虑 FGPM 板上下表面的边界条件: 在$z=-h/2$处, $\sigma_z=-q_1$, $\tau_{zx}=0$, $D_z=0$; 在$z=h/2$处, $\sigma_z=-q_2$, $\tau_{zx}=0$, $D_z=0$.

将式 (7) 和 (8) 中的σ_z, τ_{zx}和D_z的表达式代入上述边界条件, 可得到如下形式的边界条件:

$$\begin{cases} A'(\pm h/2)+1=0, \\ c_{13}(\pm h/2)+c_{33}(\pm h/2)G'(\pm h/2)+e_{33}(\pm h/2)\phi_1'(\pm h/2)=0, \\ c_{13}(\pm h/2)A(\pm h/2)+c_{33}(\pm h/2)C'(\pm h/2)+e_{33}(\pm h/2)\phi_2'(\pm h/2)=0, \\ \{c_{13}(z)[\kappa_3 F(z)+\kappa_4 B(z)]+c_{33}(z)D'(z)+e_{33}(z)\phi_0'(z)\}_{z=-h/2}=-q_1, \\ \{c_{13}(z)[\kappa_3 F(z)+\kappa_4 B(z)]+c_{33}(z)D'(z)+e_{33}(z)\phi_0'(z)\}_{z=h/2}=-q_2, \\ c_{55}(\pm h/2)[F'(\pm h/2)+G(\pm h/2)]+e_{15}(\pm h/2)\phi_1(\pm h/2)=0, \\ c_{55}(\pm h/2)[B'(\pm h/2)+C(\pm h/2)]+e_{15}(\pm h/2)\phi_2(\pm h/2)=0, \\ e_{31}(\pm h/2)+e_{33}(\pm h/2)G'(\pm h/2)-\varepsilon_{33}(\pm h/2)\phi_1'(\pm h/2)=0, \\ e_{31}(\pm h/2)A(\pm h/2)+e_{33}(\pm h/2)C'(\pm h/2)-\varepsilon_{33}(\pm h/2)\phi_2'(\pm h/2)=0, \\ e_{31}(\pm h/2)F(\pm h/2)\kappa_3+e_{31}(\pm h/2)B(\pm h/2)\kappa_4+e_{33}(\pm h/2)D'(\pm h/2)-\varepsilon_{33}(\pm h/2)\phi_0'(\pm h/2)=0. \end{cases} \tag{18}$$

若令$\bar{u}$和$\bar{w}$为板中面的位移, 即$\bar{u}(x)=u(x,0)$, $\bar{w}(x)=w(x,0)$, 由式 (5) 可得

$$A(0)=0,\ B(0)=0,\ C(0)=0,\ D(0)=0,\ F(0)=0,\ G(0)=0. \tag{19}$$

利用积分式 (9)、(13)、(14) 以及边界条件式 (18) 和关系式 (15), 可确定$A(z)$, $B(z)$, $C(z)$, $D(z)$, $F(z)$, $G(z)$, $\phi_0(z)$的表达式以及常数$\kappa_i\,(i=1,2,3,4)$, 其表达式见附录. 函数$\phi_0(z)$中的常数Φ_0与参考电势有关, 它对板中的应力和电位移无影响. 令$\phi_0(0)=0$可得Φ_0的值, 具体见附录.

2　轴力、弯矩、剪力和边界条件

利用应力表达式 (7), 可得如下板的轴力N_x、弯矩M_x和剪力Q_x的表达式:

$$N_x=\int_{-h/2}^{h/2}\sigma_x \mathrm{d}z=N_1\bar{u}_{,x}+N_3\bar{w}_{,xx}+N_5\bar{u}_{,xxx}+N_7\bar{w}_{,xxxx}+N_0, \tag{20}$$

$$M_x=\int_{-h/2}^{h/2}\sigma_x z\mathrm{d}z=M_1\bar{u}_{,x}+M_3\bar{w}_{,xx}+M_5\bar{u}_{,xxx}+M_7\bar{w}_{,xxxx}+M_0, \tag{21}$$

$$Q_x=\int_{-h/2}^{h/2}\tau_{zx}\mathrm{d}z=Q_1\bar{u}_{,xx}+Q_2\bar{w}_{,xxx}, \tag{22}$$

式中

$$\begin{cases} N_1=\int_{-h/2}^{h/2}(c_{11}+c_{13}G'+e_{31}\phi_1')\mathrm{d}z,\ N_3=\int_{-h/2}^{h/2}(c_{11}A+c_{13}C'+e_{31}\phi_2')\mathrm{d}z, \\ N_5=\int_{-h/2}^{h/2}c_{11}F\mathrm{d}z,\ N_7=\int_{-h/2}^{h/2}c_{11}B\mathrm{d}z,\ N_0=\int_{-h/2}^{h/2}(c_{13}D'+e_{31}\phi'_0)\mathrm{d}z, \\ M_1=\int_{-h/2}^{h/2}z(c_{11}+c_{13}G'+e_{31}\phi_1')\mathrm{d}z,\ M_3=\int_{-h/2}^{h/2}z(c_{11}A+c_{13}C'+e_{31}\phi_2')\mathrm{d}z, \\ M_5=\int_{-h/2}^{h/2}c_{11}zF\mathrm{d}z,\ M_7=\int_{-h/2}^{h/2}c_{11}zB\mathrm{d}z,\ M_0=\int_{-h/2}^{h/2}(c_{13}D'+e_{31}\phi')z\mathrm{d}z, \\ Q_1=\int_{-h/2}^{h/2}[c_{55}(F'+G)+e_{15}\phi_1]\mathrm{d}z,\ Q_2=\int_{-h/2}^{h/2}[c_{55}(B'+C)+e_{15}\phi_2]\mathrm{d}z. \end{cases} \tag{23}$$

本文考虑在 FGPM 板的柱面边界可以有以下类型的边界: 简支边界 (S)、第一类固支边界 (C1)、第二类固支边界 (C2) 和自由边界 (F), 即

$$\mathrm{S}:\quad \bar{u}=0,\bar{w}=0,M_x=0, \tag{24}$$

$$\mathrm{C1}:\quad \bar{u}=0,\bar{w}=0,\bar{w}_{,x}=0, \tag{25}$$

$$\mathrm{C2}:\quad \bar{u}=0,\bar{w}=0,u_{,z}=0, \tag{26}$$

$$\mathrm{F}:\quad N_x=0,M_x=0,Q_x=0. \tag{27}$$

定义横截面上的平均电位移表达式为

$$D_x^* = \frac{1}{h}\int_{-h/2}^{h/2} D_x \mathrm{d}z = D_1\bar{u}_{,xx} + D_2\bar{w}_{,xxx}, \tag{28}$$

式中

$$D_1 = \int_{-h/2}^{h/2} [e_{15}(F'+G) - \varepsilon_{11}\phi_1]\mathrm{d}z,\ D_2 = \int_{-h/2}^{h/2} [e_{15}(B'+C) - \varepsilon_{11}\phi_2]\mathrm{d}z. \tag{29}$$

令 FGPM 板柱面边界上(x=0,l)的平均电位移$D_x^* = 0$,借此可确定函数$\phi_1(z)$和$\phi_2(z)$的表达式,详见附录.

3 数值算例与分析

为方便起见,引入无量纲量$\bar{W} = \bar{w}E/(qh)$, $\bar{\sigma}_x = \sigma_x/q$和$\bar{\tau}_{zx} = \tau_{zx}/q$.

3.1 结果验证

为验证本文解答的有效性,现考虑将 FGPM 板退化为均匀材料压电板.采用商业有限元软件 ABAQUS,建立横向均布荷载$q_1 = 1\times10^6$ N/m作用下两端简支均匀压电板的有限元模型,网格单元类型为 C3D8E,取弹性模量$E = 70$ GPa, Poisson 比$\upsilon = 0.3$, 压电常数$e_{31} = -5.2$ C/m^2, $e_{33} = -15.1$ C/m^2, $e_{15} = 12.7$ C/m^2, 介电常数$\varepsilon_{11} = 6.5\times10^{-11}$ F/m, $\varepsilon_{33} = 5.6\times10^{-11}$ F/m.对比$z = 0$时的无量纲位移$\bar{W}$(见表 1)发现,本文解答与有限元模拟结果吻合情况良好,误差仅在 0.55% 以内.

表 1 $z = 0$处的无量纲位移$\bar{W}$对比

Table 1 Comparison of dimensionless displacement $\bar{W}$ at $z = 0$

x	0	0.1	0.2	0.3	0.4	0.5	0.6	0.7	0.8	0.9	1.0
this paper	0	61.162	115.183	157.221	183.821	192.924	183.819	157.223	115.184	61.159	0
FEM	0	61.164	114.669	156.379	182.810	191.863	182.822	156.384	114.670	61.164	0
errors δ/%	–	0.003	0.446	0.536	0.550	0.550	0.542	0.534	0.446	0.008	–

Navazi 等[22] 研究了功能梯度板的非线性柱面弯曲问题,本文将 FGM 弹性板结果与该文献的线性解进行了对比,结果如表 2 和表 3 所示,其中 n 为材料的梯度因子.

表 2 n=0,z=0 处的无量纲位移 w/h 对比

Table 2 Comparison of dimensionless displacement at n=0, z=0

	x	0	0.1	0.2	0.3	0.4	0.5	0.6	0.7	0.8	0.9	1.0
ref. [22]	w/h	0	0.195	0.377	0.520	0.612	0.652	0.601	0.512	0.385	0.205	0
this paper	w/h	0	0.208	0.392	0.533	0.627	0.658	0.628	0.537	0.391	0.206	0

表 3 n=10,z=0 处的无量纲位移 w/h 对比

Table 3 Comparison of dimensionless displacement at n=10, z=0

	x	0	0.1	0.2	0.3	0.4	0.5	0.6	0.7	0.8	0.9	1.0
ref. [22]	w/h	0	0.582	1.086	1.488	1.747	1.826	1.750	1.480	1.094	0.605	0
this paper	w/h	0	0.633	1.192	1.618	1.905	1.997	1.907	1.632	1.187	0.627	0

可以发现,本文解答与文献解答吻合情况良好,从而验证了本文解答的有效性.

3.2 FGPM 板条受均布荷载作用

接下来,考虑在板上表面受均布载荷$q_1 = 1\times10^6$ N/m^{2}作用的 FGPM 板.取$l = 1$ m, $h/l = 0.15$, 材料的弹性、压电和介电参数沿板厚度方向均为坐标 z 的指数函数,变化规律为

$$C_{ij} = C_{ij}^0 \mathrm{e}^{\{(z+h/2)/h\}\lambda}, \qquad i,j = 1,2,\cdots,6,$$

$$e_{ij} = e_{ij}^0 \mathrm{e}^{\{(z+h/2)/h\}\lambda}, \qquad i,j = 1,2,\cdots,6,$$

$$\varepsilon_{ij} = \varepsilon_{ij}^0 \mathrm{e}^{\{(z+h/2)/h\}\lambda}, \qquad i,j = 1,2,\cdots,6,$$

式中,C_{ij}^0, e_{ij}^0, ε_{ij}^0分别为$z = -h/2$处的材料弹性常数、压电常数和介电常数;λ为梯度因子,表示材料的不均匀程度;当$\lambda = 0$时,压电功能梯度板退化为压电均匀板.取$C_{11}^0 = 139$ GPa, $C_{33}^0 = 115$ GPa, $C_{13}^0 = 74$ GPa, $C_{55}^0 = 25.6$ GPa, $e_{31}^0 = -5.2$ C/m^2, $e_{33}^0 = -15.1$ C/m^2, $e_{15}^0 = 12.7$ C/m^2, $\varepsilon_{11}^0 = 6.5\times10^{-11}$ F/m, $\varepsilon_{33}^0 = 5.6\times10^{-11}$ F/m[23].

图 2 给出了$\lambda = -5, 0, 5$时,两端简支 FGPM 板的无量纲位移$\bar{U}$的分布,同时将相应未考虑压电效应的结果

作为对照组(图中用 FGM 板表示, 下同)进行比较. 可以发现沿厚度方向(x=0.5)的无量纲位移$\bar{U}$有明显区别, 考虑压电效应后, 无量纲位移$\bar{U}$降低了 25.46%~91.92%, 其中, 无量纲位移$\bar{U}$降低的幅度随着λ取值的增大而增大; FGPM 板和 FGM 板沿跨度方向的中面($z=0$)无量纲位移$\bar{U}$有明显区别, 考虑压电效应后, 无量纲位移$\bar{U}$降低了 17.37%~30.26%.

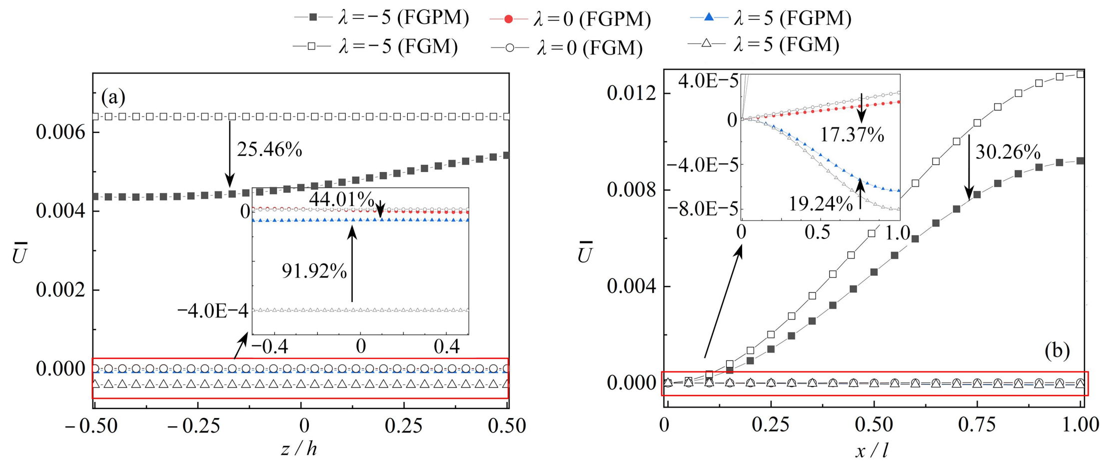

图 2　无量纲位移$\bar{U}$对比图

Fig. 2　Comparison of dimensionless displacement $\bar{U}$

图 3 给出了$\lambda=-5,0,5$时, 两端简支 FGPM 板的无量纲挠度$\bar{W}$的分布. 可以发现沿厚度方向(x=0.5)的无量纲挠度$\bar{W}$有明显区别, 考虑压电效应后, 无量纲挠度$\bar{W}$降低了 23.62%~24.93%, FGPM 板和 FGM 板沿跨度方向的中面($z=0$)无量纲挠度$\bar{W}$有明显区别, 考虑压电效应后, 无量纲挠度$\bar{W}$降低了 24.11%~27.40%.

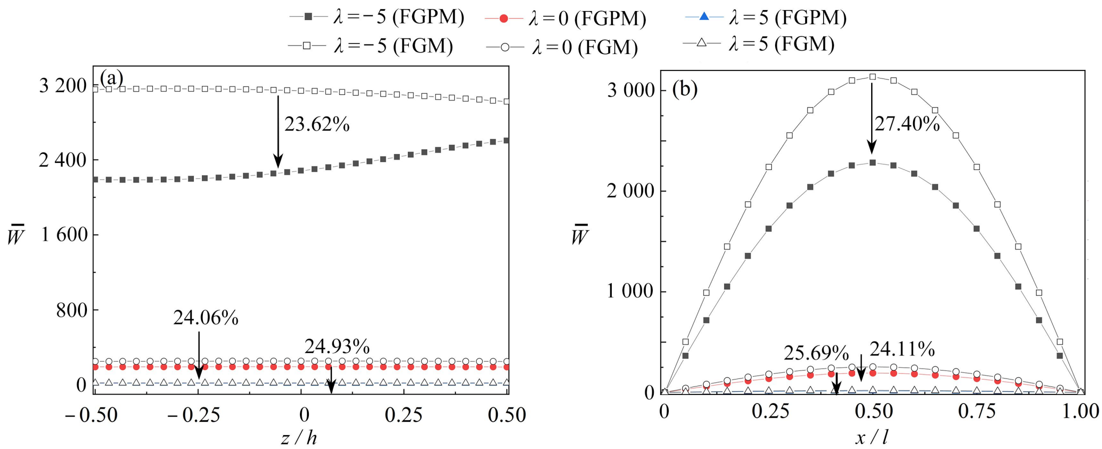

图 3　无量纲挠度$\bar{W}$对比图

Fig. 3　Comparison of dimensionless deflection $\bar{W}$

图 4 给出了$\lambda=-5,0,5$时, 两端简支 FGPM 板的无量纲正应力$\bar{\sigma}_x$和无量纲剪应力$\bar{\tau}_{xz}$的分布. 可以发现 FGPM 板和 FGM 板的无量纲正应力$\bar{\sigma}_x$(在 x=0.5 处) 和无量纲剪应力$\bar{\tau}_{xz}$(在 x=0.25 处) 分布几乎没有区别. 当考虑压电效应后, 无量纲正应力$\bar{\sigma}_x$降低范围在 0.52%~6.99%, 无量纲剪应力$\bar{\tau}_{xz}$降低范围在 0.002 2%~0.019%.

图 5 考虑了 FGPM 板在 7 种不同的边界条件和 3 种不同的λ取值的情况下, $z=0$处无量纲挠度$\bar{W}$沿x方向的分布情况. 通过比较发现, 对于这 7 种边界条件, 板的挠度值随着λ的增大而减小. 这是因为基于材料常数沿厚度方向的变化情况, 随着λ的增大, 沿厚度方向的刚度增大, 板的抗弯刚度也随之增大. 此外, 对于 S-S、C1-C1、C2-C2 边界条件, 在$x=l/2$处产生最大挠度值; 对于 C1-S、C2-S 边界条件, 其最大挠度值出现在$x=l/2$附近; 而对于 C1-F、C2-F 边界条件, 在$x=l$处产生最大挠度.

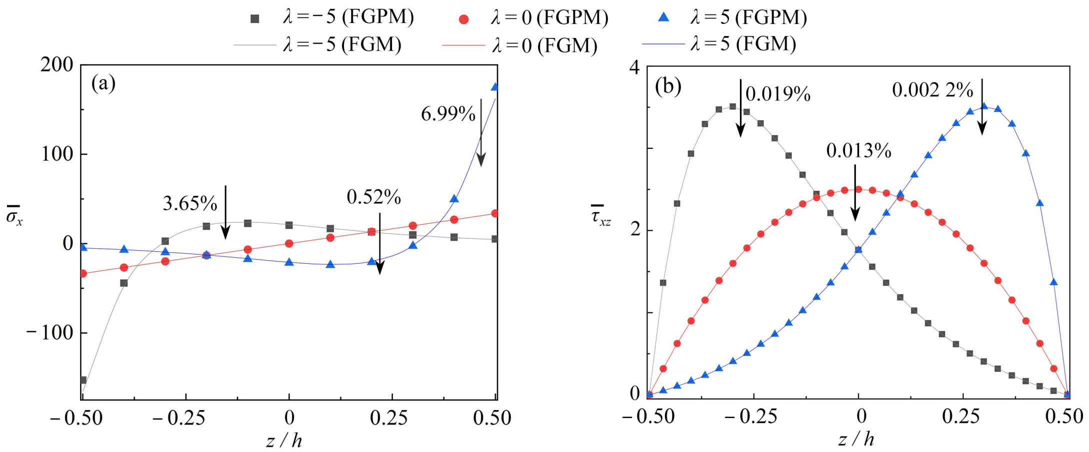

图 4　无量纲应力对比图

Fig. 4　Comparison of dimensionless stress

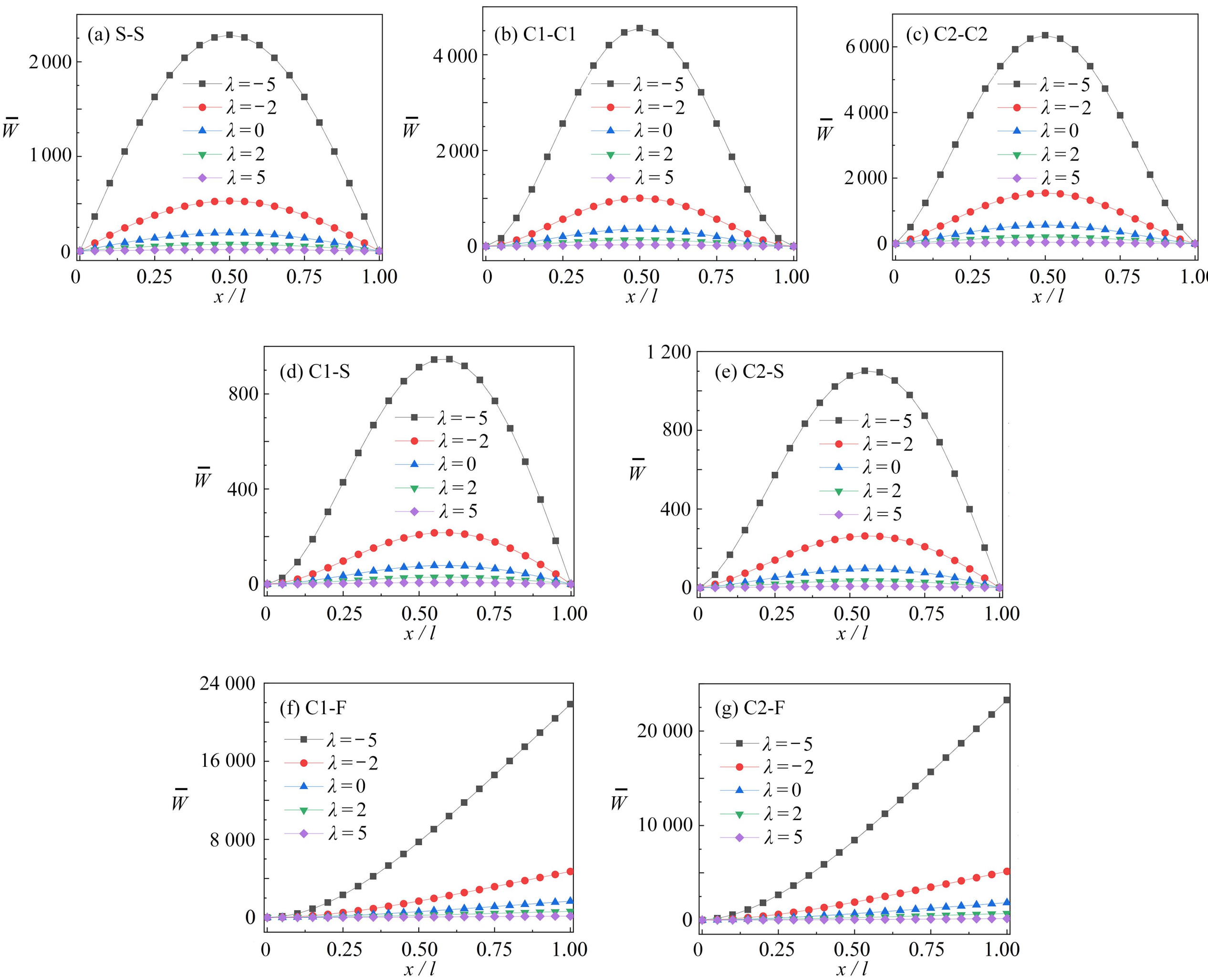

图 5　7 种边界条件下的无量纲挠度分布图

Fig. 5　Comparison of dimensionless displacement under 7 boundary conditions

4　结　　论

本文在推广后的 Mian 和 Spencer 功能梯度板理论基础上，将材料由弹性材料推广到压电材料，获得了横

向均布荷载作用下 FGPM 板柱面弯曲问题的弹性力学解, 其中, 材料梯度、压电和介电参数沿板厚方向呈任意连续变化. 通过与均匀材料压电板的数值解比较证明了本文解答的有效性. 数值算例结果表明, 边界条件和材料梯度因子对 FGPM 板柱面弯曲时的响应有显著影响, 特别是当梯度因子较大时, 易在刚度较大的表面附近产生相对较大应力. 因此, 在工程实践中, 通过调控边界条件和材料梯度因子, 可进一步控制和优化 FGPM 板静力弯曲的力学行为. 另外, 将 FGPM 板与 FGM 板进行对比可发现, 受压电效应影响, FGPM 板的无量纲位移$\bar{U}$比 FGM 板降低了 17.37%~91.92%; 无量纲挠度$\bar{W}$比功能梯度板降低了 23.62%~27.40%; 无量纲正应力$\bar{\sigma}_x$降低了 0.52%~6.99%; 无量纲剪应力τ_{xz}降幅较小, 可忽略不计. 以上结果表明通过压电效应可以调控 FGPM 板的柱面弯曲响应.

本文的理论求解体系精确满足弹性理论的基本方程和板上下表面的边界条件, 只是采用 Saint Venant 原理对板柱面边界进行了处理. 因此, 远离板柱面边界, 所得解析解可作为基准解, 用以评价在同类问题分析中采用各种近似板理论和数值解法获得的解答.

致谢　本文作者衷心感谢浙江理工大学科研启动基金 (19052460-Y) 对本文的资助.

附　录

$A(z), B(z), C(z), D(z), F(z), G(z), \phi_1(z), \phi_2(z), \phi_0(z)$的表达式为

$$\begin{cases} A(z) = -z + A_0,\ G(z) = -\int_{-h/2}^{z} \dfrac{\varepsilon_{33}c_{13} + e_{33}e_{31}}{c_{33}\varepsilon_{33} + e_{33}^2} \mathrm{d}\xi + G_0, \\ C(z) = -\int_{-h/2}^{z} \dfrac{\varepsilon_{33}c_{13} + e_{33}e_{31}}{c_{33}\varepsilon_{33} + e_{33}^2} A \mathrm{d}\xi + C_0,\ F(z) = \int_{-h/2}^{z} [(F_{10} - e_{15}\phi_1)/c_{55} - G] \mathrm{d}\xi + F_0, \\ B(z) = \int_{-h/2}^{z} [(B_{10} - e_{15}\phi_2)/c_{55} - C] \mathrm{d}\xi + B_0, \\ D(z) = -\int_{-h/2}^{z} \dfrac{\epsilon_{33}(D_{10} + D_{00}) + e_{33}(D_{20} + D_{01})}{c_{33}\epsilon_{33} + e_{33}^2} \mathrm{d}\xi + D_0, \end{cases} \tag{A1}$$

$$\begin{cases} \phi_1(z) = \int_{-h/2}^{z} \dfrac{c_{33}e_{31} - c_{13}e_{33}}{c_{33}\varepsilon_{33} + e_{33}^2} \mathrm{d}\xi + \varPhi_1,\ \phi_2(z) = \int_{-h/2}^{z} -\dfrac{c_{33}e_{31} - c_{13}e_{33}}{c_{33}\varepsilon_{33} + e_{33}^2} \xi \mathrm{d}\xi + \varPhi_2, \\ \phi_0(z) = \int_{-h/2}^{z} \dfrac{c_{33}(D_{20} + D_{01}) - e_{33}(D_{10} + D_{00})}{c_{33}\varepsilon_{33} + e_{33}^2} \mathrm{d}\xi + \varPhi_0, \end{cases} \tag{A2}$$

其中

$$A_0 = 0,\ G_0 = \int_{-h/2}^{0} \frac{\varepsilon_{33}c_{13} + e_{33}e_{31}}{c_{33}\varepsilon_{33} + e_{33}^2} \mathrm{d}\xi,\ C_0 = \int_{-h/2}^{0} -\frac{\varepsilon_{33}c_{13} + e_{33}e_{31}}{c_{33}\varepsilon_{33} + e_{33}^2} \xi \mathrm{d}\xi,$$

$$F_{10}(z) = \int_{-h/2}^{z} \left(c_{55}\kappa_1 - c_{11} - c_{13}G' - e_{31}\phi_1'\right) \mathrm{d}\xi,$$

$$F_0 = \int_{-h/2}^{0} \frac{1}{c_{55}} \left[\int_{-h/2}^{0} \left(c_{11} - c_{13}\frac{\varepsilon_{33}c_{13} + e_{33}e_{31}}{c_{33}\varepsilon_{33} + e_{33}^2}\right) \mathrm{d}\xi\right] \mathrm{d}z + \frac{h}{2}\int_{-h/2}^{0} \frac{\varepsilon_{33}c_{13} + e_{33}e_{31}}{c_{33}\varepsilon_{33} + e_{33}^2} \mathrm{d}\xi + \\ \int_{-h/2}^{0} \frac{1}{c_{55}} \left[\int_{-h/2}^{0} e_{31}\frac{c_{33}e_{31} - c_{13}e_{33}}{c_{33}\varepsilon_{33} + e_{33}^2} \mathrm{d}\xi + e_{15}\phi_1(0)\right] \mathrm{d}z - k_1 \int_{-h/2}^{0} \left(\int_{-h/2}^{0} c_{55} \mathrm{d}\xi\right) \Big/ c_{55} \cdot \mathrm{d}z - \int_{-h/2}^{0} \frac{c_{13}\varepsilon_{33} + e_{31}e_{33}}{c_{33}\varepsilon_{33} + e_{33}^2} \xi \mathrm{d}\xi,$$

$$B_{10}(z) = \int_{-h/2}^{z} (c_{55}\kappa_2 - c_{11}A - c_{13}C' - e_{31}\phi'_2) \mathrm{d}\xi,$$

$$B_0 = -\int_{-h/2}^{0} \frac{1}{c_{55}} \left[\int_{-h/2}^{0} \left(c_{11} - c_{13}\frac{\varepsilon_{33}c_{13} + e_{33}e_{31}}{c_{33}\varepsilon_{33} + e_{33}^2}\right) \xi \mathrm{d}\xi\right] \mathrm{d}z - \frac{h}{2}\int_{-h/2}^{0} \frac{\varepsilon_{33}c_{13} + e_{33}e_{31}}{c_{33}\varepsilon_{33} + e_{33}^2} \xi \mathrm{d}\xi + \\ \int_{-h/2}^{z} \frac{1}{c_{55}} \left(e_{15}\phi_2(0) - \int_{-h/2}^{0} e_{31}\frac{c_{33}e_{31} - c_{13}e_{33}}{c_{33}\varepsilon_{33} + e_{33}^2} \xi \mathrm{d}\xi\right) \mathrm{d}z - k_2 \int_{-h/2}^{0} \left(\int_{-h/2}^{0} c_{55} \mathrm{d}\xi\right) \Big/ c_{55} \cdot \mathrm{d}z - \int_{-h/2}^{0} \frac{\varepsilon_{33}c_{13} + e_{33}e_{31}}{c_{33}\varepsilon_{33} + e_{33}^2} \xi^2 \mathrm{d}\xi,$$

$$D_{10}(z) = \int_{-h/2}^{z} [c_{55}(F' + G) + (Fc_{13})' + e_{15}\phi_1]\kappa_3 + [c_{55}(B' + C) + (c_{13}B)' + e_{15}\phi_2]\kappa_4 \mathrm{d}\xi,$$

$$D_{00} = q_1 + c_{13}(-h/2)[\kappa_3 F(-h/2) + \kappa_4 B(-h/2)],$$

$$D_{20}(z) = \int_{-h/2}^{z} [e_{15}(F' + G) + (Fe_{31})' - \varepsilon_{11}\phi_1]\kappa_3 + [e_{15}(B' + C) + (e_{31}B)' - \varepsilon_{11}\phi_2]\kappa_4 \mathrm{d}\xi,$$

$$D_{01}=e_{31}(-h/2)F(-h/2)\kappa_3+e_{31}(-h/2)B(-h/2)\kappa_4,$$

$$D_0=\int_{-h/2}^{h/2}\frac{\varepsilon_{33}(D_{10}+D_{00})+e_{33}(D_{20}+D_{01})}{c_{33}\varepsilon_{33}+e_{33}^2}\mathrm{d}\xi,$$

$$\Phi_1=\int_{-h/2}^{h/2}\left[e_{15}(F'+G)-\varepsilon_{11}\int_{-h/2}^{h/2}\frac{c_{33}e_{31}-c_{13}e_{33}}{c_{33}\varepsilon_{33}+e_{33}^2}\mathrm{d}\xi\right]\mathrm{d}z\bigg/\int_{-h/2}^{h/2}\varepsilon_{11}\mathrm{d}z,$$

$$\Phi_2=\int_{-h/2}^{h/2}\left[e_{15}(B'+C)+\varepsilon_{11}\int_{-h/2}^{h/2}\frac{c_{33}e_{31}-c_{13}e_{33}}{c_{33}\varepsilon_{33}+e_{33}^2}\xi\mathrm{d}\xi\right]\mathrm{d}z\bigg/\int_{-h/2}^{h/2}\varepsilon_{11}\mathrm{d}z,$$

$$\Phi_0=\int_{-h/2}^{0}\frac{e_{33}(D_{10}+D_{00})-c_{33}(D_{20}+D_{01})}{c_{33}\varepsilon_{33}+e_{33}^2}\mathrm{d}\xi.$$

$k_i\,(i=1,2,3,4)$的表达式为

$$\begin{cases}k_1=\int_{-h/2}^{h/2}\left(c_{11}-c_{13}\frac{\varepsilon_{33}c_{13}+e_{33}e_{31}}{c_{33}\varepsilon_{33}+e_{33}^2}\right)\mathrm{d}\xi+\int_{-h/2}^{h/2}e_{31}\frac{c_{33}e_{31}-c_{13}e_{33}}{c_{33}\varepsilon_{33}+e_{33}^2}\mathrm{d}\xi\bigg/\int_{-h/2}^{h/2}c_{55}\mathrm{d}\xi,\\ k_2=-\left[\int_{-h/2}^{h/2}\left(c_{11}-c_{13}\frac{\varepsilon_{33}c_{13}+e_{33}e_{31}}{c_{33}\varepsilon_{33}+e_{33}^2}\right)\xi\mathrm{d}\xi+\int_{-h/2}^{h/2}e_{31}\frac{c_{33}e_{31}-c_{13}e_{33}}{c_{33}\varepsilon_{33}+e_{33}^2}\xi\mathrm{d}\xi\right]\bigg/\int_{-h/2}^{h/2}c_{55}\mathrm{d}\xi,\\ k_3=\frac{k_{42}}{k_{31}k_{42}-k_{32}k_{41}}(q_2-q_1),\ k_4=-\frac{k_1k_3}{k_2},\end{cases}\tag{A3}$$

其中

$$k_{31}=\int_{-h/2}^{h/2}\left[k_1\int_{-h/2}^{h/2}c_{55}\mathrm{d}\xi-\int_{-h/2}^{h/2}\left(c_{11}-c_{13}\frac{\varepsilon_{33}c_{13}+e_{33}e_{31}}{c_{33}\varepsilon_{33}+e_{33}^2}\right)\mathrm{d}\xi-\int_{-h/2}^{h/2}e_{31}\frac{c_{33}e_{31}-c_{13}e_{33}}{c_{33}\varepsilon_{33}+e_{33}^2}\mathrm{d}\xi\right]\mathrm{d}z,$$

$$k_{32}=\int_{-h/2}^{h/2}\frac{e_{15}}{c_{55}}\left[k_1\int_{-h/2}^{h/2}c_{55}\mathrm{d}\xi-\int_{-h/2}^{h/2}\left(c_{11}-c_{13}\frac{\varepsilon_{33}c_{13}+e_{33}e_{31}}{c_{33}\varepsilon_{33}+e_{33}^2}\right)\mathrm{d}\xi-\int_{-h/2}^{h/2}e_{31}\frac{c_{33}e_{31}-c_{13}e_{33}}{c_{33}\varepsilon_{33}+e_{33}^2}\mathrm{d}\xi-e_{15}\phi_1(h/2)\right]-\varepsilon_{11}\phi_1(h/2)\mathrm{d}z,$$

$$k_{41}=\int_{-h/2}^{h/2}\left[k_2\int_{-h/2}^{h/2}c_{55}\mathrm{d}\xi+\int_{-h/2}^{h/2}\left(c_{11}-c_{13}\frac{\varepsilon_{33}c_{13}+e_{33}e_{31}}{c_{33}\varepsilon_{33}+e_{33}^2}\right)\xi\mathrm{d}\xi+\int_{-h/2}^{h/2}e_{31}\frac{c_{33}e_{31}-c_{13}e_{33}}{c_{33}\varepsilon_{33}+e_{33}^2}\xi\mathrm{d}\xi\right]\mathrm{d}z,$$

$$k_{42}=\int_{-h/2}^{h/2}\frac{e_{15}}{c_{55}}\left[k_2\int_{-h/2}^{h/2}c_{55}\mathrm{d}\xi+\int_{-h/2}^{h/2}\left(c_{11}-c_{13}\frac{\varepsilon_{33}c_{13}+e_{33}e_{31}}{c_{33}\varepsilon_{33}+e_{33}^2}\right)\xi\mathrm{d}\xi+\int_{-h/2}^{h/2}e_{31}\frac{c_{33}e_{31}-c_{13}e_{33}}{c_{33}\varepsilon_{33}+e_{33}^2}\xi\mathrm{d}\xi-e_{15}\phi_2(h/2)\right]-\varepsilon_{11}\phi_2(h/2)\mathrm{d}z.$$

参考文献(References):

[1] 刘涛, 汪超, 刘庆运. 基于等几何方法的压电功能梯度板动力学及主动振动控制分析[J]. 工程力学, 2020, **37**(12): 228-242.(LIU Tao, WANG Chao, LIU Qingyun. Analysis for dynamics and active vibration control of piezoelectric functionally graded plates based on isogeometric method[J]. *Engineering Mechanics*, 2020, **37**(12): 228-242.(in Chinese))

[2] 韩杰才, 徐丽, 王保林, 等. 梯度功能材料的研究进展及展望[J]. 固体火箭技术, 2004, **27**(3): 207-215.(HAN Jiecai, XU Li, WANG Baolin, et al. Progress and prospects of functional gradient materials[J]. *Journal of Solid Rocket Technology*, 2004, **27**(3): 207-215.(in Chinese))

[3] CARL C M, WU M K, MOY K. Piezoelectric ceramics with functional gradients: a new application in material design[J]. *Journal of the American Ceramic Society*, 1996, **79**(3): 809-812.

[4] 杨博, 丁皓江, 陈伟球. 功能梯度板柱面弯曲的弹性力学解[J]. 应用数学和力学, 2008, **29**(8): 905-910.(YANG Bo, DING Haojiang, CHEN Weiqiu. Elasticity solutions for functionally graded plates in cylindrial bending[J]. *Applied Mathematics and Mechanics*, 2008, **29**(8): 905-910.(in Chinese))

[5] 边祖光. 功能梯度材料板壳结构的耦合问题研究[D]. 博士学位论文. 杭州: 浙江大学, 2005.(BIAN Zuguang. On coupled problems of functionally graded materials plates and shells[D]. PhD Thesis. Hangzhou: Zhejiang University, 2005.(in Chinese))

[6] ALMAJID A, TAYA M, HUDNUT S W, et al. Analysis of out-of-plane displacement and stress field in a piezocomposite plate with functionally graded microstructure[J]. *International Journal of Solids and Structures*, 2001,

38(19): 3377-3391.

[7] ZHONG Z, SHANG E T. Three-dimensional exact analysis of a simply supported functionally gradient piezoelectric plate[J]. *International Journal of Solids and Structures*, 2003, **40**(20): 5335-5352.

[8] NAVAZI H M, HADDADPOUR H. Nonlinear cylindrical bending analysis of shear deformable functionally graded plates under different loadings using analytical methods[J]. *International Journal of Mechanical Sciences*, 2008, **50**(12): 1650-1657.

[9] TAHANI M, MIRZABABAEE S M. Non-linear analysis of functionally graded plates in cylindrical bending under thermomechanical loadings based on a layerwise theory[J]. *European Journal of Mechanics A*: *Solids*, 2008, **28**(2): 248-256.

[10] WANG Y, XU R Q, DING H J. Analytical solutions of functionally graded piezoelectric circular plates subjected to axisymmetric loads[J]. *Acta Mechanica*, 2010, **215**(1/4): 287-305.

[11] ZHONG Z, CHEN S, SHANG E. Analytical solution of a functionally graded plate in cylindrical bending[J]. *Mechanics of Advanced Materials and Structures*, 2010, **17**(8): 595-602.

[12] 刘五祥, 仲政. 任意梯度分布功能梯度板的柱形弯曲分析[J]. 武汉理工大学学报, 2008, **30**(4): 106-109.(LIU Wuxiang, ZHONG Zheng. Analysis for functionally gradient plate of arbitrary gradient distribution in cylindrical bending[J]. *Journal of Wuhan University of Technology*, 2008, **30**(4): 106-109.(in Chinese))

[13] LI X Y, WU J, DING H J. 3D analytical solution for a functionally graded transversely isotropic piezoelectric circular plate under tension and bending[J]. *International Journal of Engineering Science*, 2011, **49**(7): 664-676.

[14] LI Y S, PAN E. Static bending and free vibration of a functionally graded piezoelectric microplate based on the modified couple-stress theory[J]. *International Journal of Engineering Science*, 2015, **97**: 40-59.

[15] ZENKOUR A M, HAFED Z S. Bending analysis of functionally graded piezoelectric plates via quasi-3D trigonometric theory[J]. *Mechanics of Advanced Materials and Structures*, 2020, **27**(18): 1551-1562.

[16] DEHSARAJI M L, SAIDI A R, MOHAMMADI M. Bending analysis of thick functionally graded piezoelectric rectangular plates using higher-order shear and normal deformable plate theory[J]. *Structural Engineering and Mechanics*, 2020, **73**(3): 259-269.

[17] 王平远, 李成, 姚林泉. 基于非局部应变梯度理论功能梯度纳米板的弯曲和屈曲研究[J]. 应用数学和力学, 2021, **42**(1): 15-26.(WANG Pingyuan, LI Cheng, YAO Linquan. Bending and buckling of functionally graded nanoplates based on the nonlocal strain gradient theory[J]. *Applied Mathematics and Mechanics*, 2021, **42**(1): 15-26.(in Chinese))

[18] 刘旭, 姚林泉. 热环境中旋转功能梯度纳米环板的振动分析[J]. 应用数学和力学, 2020, **41**(11): 1224-1236.(LIU Xu, YAO Linquan. Vibration analysis of rotating functionally gradient nanocycle plates in thermal environment[J]. *Applied Mathematics and Mechanics*, 2020, **41**(11): 1224-1236.(in Chinese))

[19] MIAN M A, SPENCER A J M. Exact solutions for functionally graded and laminated elastic materials[J]. *Journal of the Mechanics and Physics of Solids*, 1998, **46**(12): 2283-2295.

[20] 孙烨丽, 沈璐璐, 杨博. 功能梯度板中Griffith裂纹尖端应力场的三维解析研究[J]. 应用数学和力学, 2021, **42**(1): 36-48.(SUN Yeli, SHEN Lulu, YANG Bo. 3D analytical study of stress field at Griffith crack tip in functionally graded plates[J]. *Applied Mathematics and Mechanics*, 2021, **42**(1): 36-48.(in Chinese))

[21] 仲政, 尚尔涛. 功能梯度热释电材料矩形板的三维精确分析[J]. 力学学报, 2003, **35**(5): 542-552.(ZHONG Zheng, SHANG Ertao. Three dimensional exact analysis of functionally gradient piezothermoelectric material rectangular plate[J]. *Acta Mechanica*, 2003, **35**(5): 542-552.(in Chinese))

[22] NAVAZI H M, HADDADPOUR H, RASEKH M. An analytical solution for nonlinear cylindrical bending of functionally graded plates[J]. *Thin-Walled Structures*, 2006, **44**(11): 1129-1137.

[23] 柳彬彬. 功能梯度压电材料矩形板热-电-机械耦合三维分析[D]. 硕士学位论文. 合肥: 合肥工业大学, 2007.(LIU Binbin. Three dimensional analysis of thero-meehanical-electric behaviour of functionally gradient piezoelectric material rectangular plate[D]. Maste Thesis. Hefei: Hefei University of Technology, 2007. (in Chinese))